AIP | Applied Physics Letters

Identification of nitrogen acceptor in Cu2O: First-principles study

Jiraroj T-Thienprasert and Sukit Limpijumnong

Citation: Applied Physics Letters **107**, 221905 (2015); doi: 10.1063/1.4936760
View online: http://dx.doi.org/10.1063/1.4936760
View Table of Contents: http://scitation.aip.org/content/aip/journal/apl/107/22?ver=pdfcov
Published by the AIP Publishing

Identification of nitrogen acceptor in Cu_2O: First-principles study

Jiraroj T-Thienprasert[1,a)] and Sukit Limpijumnong[2,b)]
[1]*Department of Physics, Faculty of Science, Kasetsart University, Bangkok 10900, Thailand*
[2]*School of Physics and NANOTEC-SUT Center of Excellence on Advanced Functional Nanomaterials, Suranaree University of Technology, Nakhon Ratchasima 30000, Thailand*

(Received 12 August 2015; accepted 16 November 2015; published online 30 November 2015)

The source of *p*-type carriers observed in nitrogen-doped Cu_2O samples [Appl. Phys. Lett. **82**, 1060 (2003)] was identified by using accurate hybrid density functional calculations. Similar to the case of ZnO, we found that N is a deep acceptor when substituting for O in Cu_2O and cannot be the source of the observed *p*-type carriers. Detailed investigation of other N-related defects in Cu_2O reveals that N_2 substitution for Cu, i.e., $(N_2)_{Cu}$, is a shallow acceptor and can give hole carriers in N-doped Cu_2O samples. $(N_2)_{Cu}$ is not only a shallow acceptor but it also has a lower formation energy than N_O in some growth conditions. The calculated emission photo luminescence (PL) peak at 1.89 eV associated with $(N_2)_{Cu}$ is also in good agreement with the observed N-related PL peak at ~1.82 eV in N-doped Cu_2O sample. To aid future identification by Raman spectroscopy techniques, the vibrational frequencies of N_2 on both Cu and O sites were calculated. © *2015 AIP Publishing LLC*. [http://dx.doi.org/10.1063/1.4936760]

Cuprous oxide (Cu_2O) is of current interest due to its very high absorption coefficient in the visible light region, making it suitable for photovoltaic applications.[1–3] Cu_2O is an inherent *p*-type semiconductor with a direct band gap of ~2.17 eV.[4] The source of intrinsic *p*-type in this material has been assigned to Cu vacancy (V_{Cu})[5–7] which has two potentially stable forms, i.e., the symmetric (V_{Cu}) and the split vacancy ($V_{Cu\text{-}split}$). By using first-principles calculations with a generalized gradient approximation (GGA), Raebiger *et al.*[6] reported that the formation energy of V_{Cu} was lower than that of $V_{Cu\text{-}split}$ by ~0.3 eV, and the transition levels of these two forms of vacancies are both located at ~0.28 eV above the valence band maximum. However, their calculated band gap of Cu_2O is lower than that of the experimental value due to a well-known density functional theory (DFT) problem. This raises a concern on the reliability of the calculated defect transition levels as well as the defect formation energies. Recently, hybrid-functional method proposed by Heyd-Scuseria-Ernzerhof (HSE) is one of the most accepted approaches to remedy the band gap errors. By using the HSE-functional, Scanlon *et al.*[5] reported that V_{Cu} and $V_{Cu\text{-}split}$ have almost equal formation energies [E(V_{Cu}) is higher than E($V_{Cu\text{-}split}$) by only 0.01 eV] and the defect transition levels for V_{Cu} and $V_{Cu\text{-}split}$ are quite different, i.e., they are 0.22 and 0.47 eV above the valence band maximum (VBM) for V_{Cu} and $V_{Cu\text{-}split}$, respectively.[5] These calculated transition levels are in good agreement with the trap levels at 0.2 and 0.5 eV observed in the deep-level transient spectroscopy (DLTS) studies.[8]

Undoped Cu_2O samples have too low hole concentrations for photovoltaic applications. Several low-cost crystal growth methods to improve the hole concentration in Cu_2O samples have been proposed.[2,3,9] Doping by group V elements, especially by nitrogen, is one of the leading approaches. The observed hole concentrations in N-doped Cu_2O samples are in the order of 10^{15}–10^{18} cm^{-3} with the activation energy of ~140 meV.[9–11] These hole concentrations can be further enhanced up to two orders of magnitude by exposing the N-doped Cu_2O sample to hydrogen plasma.[2,3,9] Ishizuka *et al.*[3] have attributed the increasing of the hole concentrations to the passivation of Cu dangling bonds by hydrogen. N-doped Cu_2O samples show a strong N-related photoluminescence (PL) peak centered at ~680 nm (~1.82 eV) after hydrogen treatment.[2,3,9] Nitrogen atoms are generally believed to substitute on the oxygen sites (N_O). Recently, Zhao *et al.*[12] studied the effect of N_O on electronic structure and optical properties of Cu_2O by using the DFT-GGA.[12] They reported that N_O slightly widens the band gap and forms an intermediate band in the gap at ~0.9 eV from the VBM. Our calculated results based on HSE functional also reveal that N_O is a deep acceptor with an activation energy of ~0.53 eV. Despite the difference in the calculated values of the acceptor level, both Zhao *et al.*[12] and us found N_O to be a deep acceptor; making it unlikely to be the cause of the experimentally observed holes as widely believed. (This is similar to the case of N_O in ZnO, where N_O is also a deep acceptor[13–16] and cannot give a significant amount of holes.) Therefore, there must be another form of N-related defect that is a shallow acceptor in N-doped Cu_2O.

In this paper, we focus our attentions on N-related defects in Cu_2O that can be the source of experimentally observed shallow acceptors, by using first-principles hybrid density functional calculations. In addition to N-related defects, dominant native defects in Cu_2O, i.e., V_{Cu} and $V_{Cu\text{-}split}$, were also studied for systematic comparisons. We will show that (1) N_O defect is a deep acceptor and cannot be the source of the hole carriers observed in N-doped Cu_2O samples, (2) N_2 on Cu's site $(N_2)_{Cu}$ is a shallow acceptor with a very low formation energy under Cu-poor growth condition, making it a plausible source of the observed hole carriers in N-doped Cu_2O sample, and (3) the experimentally observed N-related PL peak at 1.82 eV in N-doped Cu_2O

a)fscicwt@ku.ac.th
b)sukit@sut.ac.th

samples[2,3,9] is consistent with our calculated PL emission peak of 1.89 eV associated with $(N_2)_{Cu}$.

We used first-principles calculations based on density functional theory with a plane-wave basis set as implemented in the VASP code.[17] The interactions between core and valence electrons were described by the projector augmented-wave (PAW) method.[18] The energy cutoff for expanding the plane wave basis set was set at 400 eV. For the exchange-correlation energy, the screened hybrid functional proposed by HSE[19] was employed to remedy the band gap problems. In the HSE functional, the amount of nonlocal Fock-exchange was set at 27.5%; following Scanlon *et al.*[5,20] With this setting, we calculated the cuprite Cu_2O the unit cell of which is composed of four Cu atoms and two O atoms with space-group $Pn\bar{3}m$. While each Cu atom is linearly connected with two O atoms, each O atom is surrounded by 4 Cu atoms. The calculated lattice constant of 4.29 Å is in good agreement with the experimental value of 4.27 Å.[21] The calculated band gap of 2.11 eV is also in good agreement with the experimental band gap of 2.17 eV.[22] To study defects in Cu_2O, we used the supercell approach with a supercell size of 96-atom, which is sufficient to suppress fictitious periodic interactions between defects in adjacent supercells.[23] For k-space integrations, the Monkhorst-Pack scheme[24] was used with a sampling k-points mesh of $5 \times 5 \times 5$ for bulk calculation. For supercell calculations, a single non-gamma special k-point (0.5, 0.5, 0.5), equivalent to 16 k-points in the bulk, was used. All atoms in the supercell were allowed to relax until all forces became less than 2×10^{-2} eV/Å. The likelihood of defect formation and its stability could be determined from its formation energy defined by[23]

$$\Delta H_f(D^q) = E_{tot}(D^q) - E_{tot}(bulk) + \sum n_i \mu_i + q(E_F + E_{VBM}), \quad (1)$$

where the first and the second terms are the total energies of a supercell containing the defect D in charge state q and that of a defect-free supercell, respectively. n is the number of atom species i which is removed from (or added to, if negative) a supercell to create the defect D, μ is the atomic chemical potential of atom species i described below, q is the charge state of the defect (the number of electrons or holes exchanged), and E_F is the Fermi-level referenced to the VBM. The lower defect formation energy means the defect is more likely to form.

To grow Cu_2O under thermodynamic equilibrium, it is required that the following condition must be satisfied:

$$E_{tot}(Cu_2O) = 2\mu_{Cu} + \mu_O, \quad (2)$$

where $E_{tot}(Cu_2O)$ is the total energy per formula unit of Cu_2O, μ_{Cu} and μ_O are the chemical potentials for Cu and O atoms, respectively. If the sum on the right-hand side of Eq. (2) is larger than $E_{tot}(Cu_2O)$, the growth process will take place rapidly and a high quality crystal would not be achieved. If the sum is less than E_{tot} (Cu_2O), the crystal will be disintegrated. There are additional conditions needed to prevent unwanted phases, such as CuO, metallic Cu, or O_2, to form. These conditions limit the ranges of possible μ_{Cu} and μ_O in addition to the relationship between the two defined in Eq. (2). Two extreme chemical potential limits, i.e., the Cu-rich and O-rich (Cu-poor) conditions will be used to present our results. For Cu-rich growth condition, we set μ_{Cu} to the total energy of Cu metallic phase. In this case, μ_O is simply determined from Eq. (2), i.e., $\mu_O = E_{tot}(Cu_2O) - 2\mu_{Cu}$. For O-rich (Cu-poor) growth condition, μ_O is set to half the total energy of an O_2 molecule, i.e., $\mu_O = E_{tot}(O_2)/2$. In this case, μ_{Cu} is limited by the CuO phase, i.e., $\mu_{Cu} = E_{tot}(CuO) - \mu_O$. For N, to prevent the formation of Cu_3N phase, μ_N has to be limited by Cu_3N phase under both Cu-rich and O-rich growth conditions, i.e., $\mu_N = E_{tot}(Cu_3N) - 3\mu_{Cu}$. Our calculated total energy per formula unit for Cu, O_2, N_2, Cu_2O, CuO, and Cu_3N are −4.13, −8.89, −11.73, −18.74, −14.46, and −23.46 eV, respectively.

For single-N defects, we studied N interstitial (N_i) and N substitutional on oxygen (N_O). The formation energies of these N-related defects as a function of Fermi energy under Cu-rich and Cu-poor growth conditions are shown in Fig. 1. For N_i, we explored three plausible configurations for N to incorporate, i.e., (1) addition of N on the tetrahedral interstitial site (N_i^{tet}), (2) on the octahedral interstitial site (N_i^{oct}), and (3) a split interstitial N labeled as $(NO)_{split}$—an additional N forming a strong bond with a lattice O atom and sharing the O site. All of these interstitial N have quite high formation energy under both Cu-rich and Cu-poor growth conditions, reflecting that they will form in an insignificant amount. On the other hand, nitrogen substitution for O, i.e., N_O, has a low formation energy under both Cu-rich and Cu-poor growth conditions. It has a defect transition level at $\varepsilon(0/-1) = 0.53$ eV; indicating that it is a deep acceptor. Therefore, N_O cannot be the source of the shallow hole (activation energy of ∼0.14 eV) observed experimentally in N-doped Cu_2O samples.[9,10] This is similar to the case of N_O in N-doped ZnO, which also produces a deep level in the ZnO band gap and could not give shallow holes.[16] The reasons that N substitution for O is not a shallow defect were extensively discussed for the case of ZnO[13,14,16,25] and can be applied for the case at hand.

Ishizuka *et al.*[2,3,9] have also reported that N-doped Cu_2O sample shows an N-related PL peak centered at

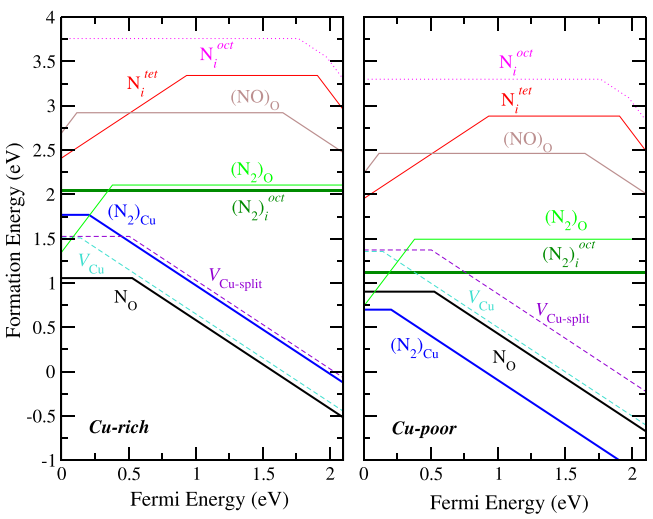

FIG. 1. Formation energy of N-related defects as a function of Fermi energy under Cu-rich and Cu-poor growth conditions.

~1.82 eV which is enhanced after a hydrogen treatment due to the passivation of non-radiative recombination centers. To compare with the experimental result, we calculated the optical absorption and emission energies associated with N_O defect by using the method described in Ref. 16. In Fig. 2 right panel, a schematic illustration of the PL process between the two electronic states of N_O is shown. The local structure of N_O defect with its hole density is shown in the left panel. We obtained the calculated emission energy of 1.568 eV. This is consistent with a deep level character of N_O but is much lower than that of the observed PL peak of 1.82 eV. Because the calculated hole activation energy and optical emission energy of N_O are very different from the experiment, the source of holes observed in the experiments must come from another N-related defect in Cu_2O.

It has been reported that N_2 on Zn vacancy defect in ZnO could be responsible for *p*-type conductivity in ZnO.[13,26] For the same reasons, dimer N_2 defects are also likely to form in Cu_2O. Therefore, we investigated three plausible types of N_2-related defects in Cu_2O, i.e., (1) interstitial N_2, (2) N_2 at the O site, and (3) N_2 at the Cu site, to seek for the source of the observed hole carriers in Cu_2O. (1) For $(N_2)_i$, our calculations show that N_2 is charge neutral and, as an interstitial defect, it prefers to occupy at the octahedral site $(N_2)_i^{oct}$ over the tetragonal site (not shown in the plot) with the energy difference of ~0.9 eV. This is partly because the octahedral site has more space to accommodate the N_2 molecule than the tetragonal site. The formation energy of an interstitial N_2 is quite high, especially under the Cu-rich growth condition. The formation energy turns slightly lower under Cu-poor growth condition but still higher than that of N_O. (2) N_2 substituted on O's site $(N_2)_O$ is a deep double donor with the transition levels at $\varepsilon(+2/0) = 0.38$ eV. The formation energy of $(N_2)_O$ is almost always higher than that of N_O under both Cu-rich and Cu-poor growth conditions. Therefore, $(N_2)_i$ and $(N_2)_O$ are unlikely to form in a significant amount due to their relatively high formation energies. Even if they are formed, they would not provide shallow holes. (3) Interestingly, N_2 substituted on the Cu site $(N_2)_{Cu}$ is an acceptor with a shallow transition level at 0.20 eV as shown in Fig. 1, making it a possible source of hole carriers. To verify that the acceptor level of $(N_2)_{Cu}$ has actual shallow characteristic, we calculated its charge (hole) density and found that the density is delocalized around N_2 similar to the case of V_{Cu}.[27] Therefore, the acceptor state of $(N_2)_{Cu}$ behaves like that of V_{Cu} which has a delocalized perturbed valence-band-like state,[6,27] confirming its shallow nature. Although, $(N_2)_{Cu}$ is not the lowest energy defect under Cu-rich growth condition, it becomes the lowest-energy defect under Cu-poor growth condition (see Fig. 1); indicating that $(N_2)_{Cu}$ is more favorable than N_O. We further investigated the stability of $(N_2)_{Cu}$ by calculating its binding energy using $(N_2)_i$ and V_{Cu} as the two parent defects and found that the reaction $(N_2)_i + V_{Cu} \rightarrow (N_2)_{Cu}$ is exothermic with the binding energy of 1.7 eV which is very large, making $(N_2)_{Cu}$ highly stable.

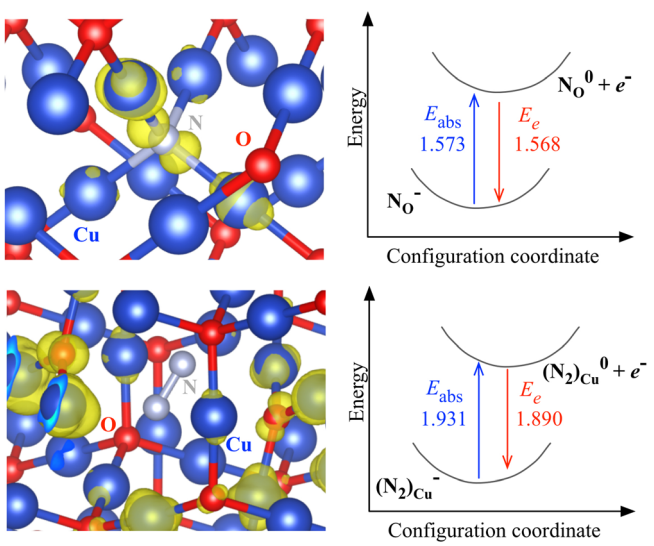

FIG. 2. (Top left) The local structure of N_O^0 with the charge (hole) density associated with the deep acceptor level shown. (Top right) The schematic illustration of the calculated optical absorption (E_{abs}) and emission (E_e) energies associated with N_O defect for exchanging an electron with the conduction band. The bottom panel shows the local structure, charge density and optical absorption and emission for $(N_2)_{Cu}$.

To compare with the experimentally observed PL peak,[2,3,9] the optical absorption and emission spectra associated with $(N_2)_{Cu}$ were calculated (Fig. 2, lower panel) using the approached described by Van de Walle and Neugebauer.[23] This was carried out by assuming that the optical process, i.e., the photon absorption or emission, is taking place much faster than the atomic relaxation. That is when an electron of $(N_2)_{Cu}^{1-}$ is excited to the conduction band by absorbing a photon, i.e., $(N_2)_{Cu}^{1-} + \text{photon} \rightarrow (N_2)_{Cu}^{0} + e^-$, the configuration coordinates of the final state $(N_2)_{Cu}^{0}$ remain the same as that of $(N_2)_{Cu}^{1-}$. Such absorption process is schematically illustrated using a vertical blue line in Fig. 2. Note that the final state right after the excitation is not the lowest energy configuration of $(N_2)_{Cu}^{0}$. It will later relax without any barrier to the lowest energy configuration. When an electron is recombined with $(N_2)_{Cu}^{0}$ and emitted a photon, i.e., $(N_2)_{Cu}^{0} + e^- \rightarrow (N_2)_{Cu}^{1-} + \text{photon}$, $(N_2)_{Cu}^{1-}$ also remains in the same configuration as that of the initial $(N_2)_{Cu}^{0}$, illustrated by a vertical red line in Fig. 2. The calculated optical emission peak of 1.89 eV is in good agreement with the experimental PL peak at 1.82 eV.[2,3,9] To aid future identification of $(N_2)_{Cu}$ by Raman spectroscopy techniques, the localized stretching vibrational mode (LVM) associated with N_2 on Cu's as well as O's sites were calculated (Table I) by using the approach described in Ref. 28. In this approach, we calculated the total energy changes as the N_2 bond distance is compressed and extended at several small steps. Then, the calculated energy vs displacement data set is fitted with the fourth degree polynomial, i.e., $V(x) = (1/2)kx^2 + \alpha x^3 + \beta x^4$; resulting in the values of k, α, and β. From the potential function, the vibrational frequency including the anharmonic contributions can be calculated. By calibrating the calculated LVM with the known value of N_2 free molecule of 2359 cm^{-1},[29] we found that the calculated value is 6.7% larger than the actual value. To correct for this systematic error, the last column of Table I shows the 6.7%-reduced LVM of each defect. The calculated LVMs of N_2 on Cu's and O's sites differ by ~400 cm^{-1}; making it easy to distinguish between the two. Note that the LVM of the two charge states of $(N_2)_{Cu}$ are virtually the

TABLE I. Calculated local stretching vibrational modes (LVM) of N_2 free molecule and N_2 defect on Cu's and O's sites.

Type	Bond length (Å)	Calculated LVM (cm^{-1})	Corrected LVM (cm^{-1})[a]
N_2 molecule	1.106	2528	2359
$(N_2)_{Cu}^{0}$	1.108	2444	2280
$(N_2)_{Cu}^{-1}$	1.109	2444	2280
$(N_2)_{O}^{0}$	1.150	2067	1929
$(N_2)_{O}^{-1}$	1.286	1403	1309

[a]Scaled down by 6.7% from the calculated LVM to adjust for the systematic errors.

same; indicating that the additional electron is not localized on the N_2—another sign that the hole state is not a localized deep state. On the other hand, for $(N_2)_O$, the state is a localized deep state and the two charge states have very distinct LVMs due to the difference in the amount of electrons participating in the N_2 bonds.

In conclusion, various plausible nitrogen configurations in Cu_2O were studied by using first-principles DFT calculations with HSE functional to identify the source of the hole carriers observed experimentally in N-doped Cu_2O samples. Consistent with prior calculations by another group, our results showed that N_O defect in Cu_2O is a deep acceptor and cannot be the source of the experimentally observed hole carrier. We found that N_2 on Cu's site is, however, a shallow acceptor and energetically more favorable to form than N_O under Cu-poor growth conditions. In addition, $(N_2)_{Cu}$ has a calculated emission PL peak at 1.89 eV which is in good agreement with the experimentally observed N-related PL peak at ~1.82 eV in the N-doped Cu_2O samples. Therefore, we assigned $(N_2)_{Cu}$ to be the source of the observed hole in N-doped Cu_2O. To aid future experimental identification of $(N_2)_{Cu}$, we calculated the local vibrational frequencies of $(N_2)_{Cu}$ and obtained the value of 2280 cm^{-1}, which could be used for comparing with results from Raman spectroscopy measurements.

One of the authors (J.T.) was supported by TRF (Grant No. 5780259), KURDI (Grant No. M-V13.57) and Stimulus Research Fund from Faculty of Science, Kasetsart University. Another author (S.L.) was supported by NANOTEC-SUT Center of Excellence on Advanced Functional Nanomaterials. Computations were carried out at the Synchrotron Light Research Institute (Public Organization), Thailand.

[1]W.-C. Huang, L.-M. Lyu, Y.-C. Yang, and M. H. Huang, J. Am. Chem. Soc. **134**, 1261 (2012); F. Caballero-Briones, J. M. Artes, I. Díez-Pe'rez, P. Gorostiza, and F. Sanz, J. Phys. Chem. C **113**, 1028 (2009); A. Mittiga, E. Salza, F. Sarto, M. Tucci, and R. Vasanthi, Appl. Phys. Lett. **88**, 163502 (2006); T. Mahalingam, J. S. P. Chitra, S. Rajendran, M. Jayachandran, and M. J. Chockalingam, J. Cryst. Growth **216**, 304 (2000); A. O. Musa, T. Akomolafe, and M. J. Carter, Sol. Energy Mater. Sol. Cells **51**, 305 (1998); W. Siripala, L. D. R. D. Perera, K. T. L. DeSilva, J. K. D. S. Jayanetti, and I. M. Dharmadasa, *ibid.* **44**, 251 (1996); L. C. Olsen, F. W. Addis, and W. Miller, Sol. Cells **7**, 247 (1982); G. P. Pollack and D. Trivich, J. Appl. Phys. **46**, 163 (1975); T. Minami, Y. Nishi, T. Miyata, and J.-I. Nomoto, Appl. Phys. Express **4**, 062301 (2011).
[2]S. Ishizuka, S. Kato, Y. Okamoto, T. Sakurai, K. Akimoto, N. Fujiwara, and H. Kobayashi, Appl. Surf. Sci. **216**, 94 (2003).
[3]S. Ishizuka, S. Kato, Y. Okamoto, and K. Akimoto, J. Cryst. Growth **237**, 616 (2002).
[4]A. Onsten, M. Mansson, T. Claesson, T. Muro, T. Matsushita, T. Nakamura, T. Kinoshita, U. O. Karlsson, and O. Tjernberg, Phys. Rev. B **76**, 115127 (2007).
[5]D. O. Scanlon, B. J. Morgan, G. W. Watson, and A. Walsh, Phys. Rev. Lett. **103**, 096405 (2009).
[6]H. Raebiger, S. Lany, and A. Zunger, Phys. Rev. B **76**, 045209 (2007).
[7]A. F. Wright and J. S. Nelson, J. Appl. Phys. **92**, 5849 (2002).
[8]G. K. Paul, R. Ghosh, S. K. Bera, S. Bandyopadhyay, T. Sakurai, and K. Akimoto, Chem. Phys. Lett. **463**, 117 (2008); G. K. Paul, Y. Nawa, H. Sato, T. Sakurai, and K. Akimoto, Appl. Phys. Lett. **88**, 141901 (2006).
[9]Y. Okamoto, S. Ishizuka, S. Kato, T. Sakurai, N. Fujiwara, H. Kobayashi, and K. Akimoto, Appl. Phys. Lett. **82**, 1060 (2003).
[10]S. Ishizuka, S. Kato, T. Maruyama, and K. Akimoto, Jpn. J. Appl. Phys., Part 1 **40**, 2765 (2001); S. Ishizuka, T. Maruyama, and K. Akimoto, Jpn. J. Appl. Phys., Part 2 **39**, L786 (2000).
[11]C. Malerba, C. L. Azanza Ricardo, M. D'Incau, F. Biccari, P. Scardi, and A. Mittiga, Sol. Energy Mater. Sol. Cells **105**, 192 (2012).
[12]Z. Zhao, X. He, J. Yi, C. Ma, Y. Cao, and J. Qiu, RSC Adv. **3**, 84 (2013).
[13]A. Boonchun and W. R. L. Lambrecht, Phys. Status Solidi B **250**, 2091 (2013).
[14]M. C. Tarun, M. Z. Iqbal, and M. D. McCluskey, AIP Adv. **1**, 022105 (2011).
[15]S. Lautenschlaeger, M. Hofmann, S. Eisermann, G. Haas, M. Pinnisch, A. Laufer, and B. K. Meyer, Phys. Status Solidi B **248**, 1217 (2011).
[16]J. L. Lyons, A. Janotti, and C. G. Van de Walle, Appl. Phys. Lett. **95**, 252105 (2009).
[17]G. Kresse and J. Hafner, J. Phys.:Condens. Matter **6**, 8245 (1994); G. Kresse and J. Furthmüller, Comp. Mater. Sci. **6**, 15 (1996); G. Kresse and D. Joubert, Phys. Rev. B **59**, 1758 (1999).
[18]P. E. Blöchl, Phys. Rev. B **50**, 17953 (1994).
[19]J. Heyd, G. E. Scuseria, and M. Ernzerhof, J. Chem. Phys. **118**, 8207 (2003).
[20]D. O. Scanlon and G. W. Watson, Phys. Rev. Lett. **106**, 186403 (2011).
[21]A. Werner and H. D. Hochheimer, Phys. Rev. B **25**, 5929 (1982); J. Ghijsen, L. H. Tjeng, J. van Elp, H. Eskes, J. Westerink, G. A. Sawatzky, and M. T. Czyzyk, *ibid.* **38**, 11322 (1988).
[22]S. N. Kale, S. B. Ogale, S. R. Shinde, M. Sahasrabuddhe, V. N. Kulkarni, R. L. Greene, and T. Venkatesan, Appl. Phys. Lett. **82**, 2100 (2003).
[23]C. G. Van de Walle and J. Neugebauer, J. Appl. Phys. **95**, 3851 (2004).
[24]H. J. Monkhorst and J. D. Pack, Phys. Rev. B **13**, 5188 (1976).
[25]S. J. Jokela and M. D. McCluskey, J. Appl. Phys. **107**, 113536 (2010).
[26]W. R. L. Lambrecht and A. Boonchun, Phys. Rev. B **87**, 195207 (2013).
[27]A. Soon, X. Y. Cui, B. Delley, S. H. Wei, and C. Stampfl, Phys. Rev. B **79**, 035205 (2009).
[28]S. Limpijumnong, J. E. Northrup, and C. G. Van de Walle, Phys. Rev. B **68**, 075206 (2003).
[29]NIST Computational Chemistry Comparison and Benchmark Database, NIST Standard Reference Database Number 101, Release 16a, August 2013, edited by R. D. Johnson III, URL: http://cccbdb.nist.gov/.